# A Low-Power System Design for Lamb Wave Methods

Shaver Deyerle[a], Dong Sam Ha[a], and Daniel J. Inman[b]
[a]Center for Embedded Systems for Critical Applications (CESCA)
Department of Electrical and Computer Engineering, Virginia Tech, Blacksburg, VA 24061
[b]Center for Intelligent Material Systems and Structures (CIMSS)
Virginia Tech, 310 Durham Hall MC 0261, Blacksburg, VA 24061

## ABSTRACT

The analog-to-digital converter (ADC) of a Lamb wave system samples a response signal and converts it into a digital signal for further processing in the digital domain. A typical ADC used for a Lamb wave system consumes a large amount of power. It also increases the complexity of the signal processing for the processor, which, in turn, increases the power consumption of the processor. Elimination of the ADC can therefore significantly reduce the overall power dissipation of a Lamb wave system. In this paper, we propose a method to eliminate the ADC of a Lamb wave system, in which the ADC is replaced by two comparators. Our method quantizes the sampled signal into three levels rather than $2^n$ levels as with an n-bit ADC. The experimental results performed with our prototype indicate that the proposed method is effective at detecting simulated damage on aluminum plates.

**Keywords:** Low power SHM system, Low power Lamb wave system, Lamb Wave, Analog-to-digital converter, ADC, Comparator

## 1 INTRODUCTION

Wireless structural health monitoring (SHM) systems are highly desirable, and a key requirement for a wireless system is low power dissipation. Lamb wave methods typically require high speed and high resolution analog-to-digital converters (ADCs) to convert response signals into the digital domain, where they are processed by a general purpose processor, digital signal processor (DSP), or microcontroller unit (MCU). Such high speed ADCs consume a significant amount of power. For example, our Lamb wave prototype uses an ADC with a sampling rate of 8.3 Mega Samples per Second (MSPS) and a resolution of 12 bits, while dissipating over 120 mW [1]. In addition, the large amount of sampled data generated by the ADC requires a high speed processor, leading to even higher power consumption. In this paper, we present a new Lamb wave method which eliminates ADCs to save power. Our method replaces the ADC of a Lamb wave system with two comparators. A comparator is functionally equivalent to a 1-bit ADC, but the circuit complexity and power requirements are significantly lower. In addition, the required signal processing is drastically simplified, which, in turn, reduces the power consumption of the processor.

This paper is organized as follows: Section 2 reviews existing Lamb wave systems including our previous system. Section 3 discusses our proposed method, Section 4 presents our prototype and experimental results, and Section 5 concludes the paper.

## 2 PRELIMINARIES

### 2.1 Review of Existing Methods

A Lamb wave SHM system uses a piezoelectric transducer, specifically a PZT (Lead Zirconate Titanate) patch, to launch an elastic wave into a structure, and the response signal is sensed by the same PZT patch or another attached somewhere else on the structure [2, 3]. A self-contained Lamb wave system typically comprises three functional blocks: a signal processing block, a signal actuation block, and a signal sensing block. The signal processing block is based on a general purpose processor, a digital signal processer (DSP) chip, or a microcontroller unit (MCU). The signal actuation block is comprised of a digital-to-analog converter (DAC), which generates an analog signal from a waveform stored in memory. This analog signal is then amplified and applied to a PZT patch attached to the structure. The response signal picked up by a PZT patch is usually amplified, sampled, and digitized by an ADC. Finally, the signal processing block processes

Health Monitoring of Structural and Biological Systems 2010, edited by Tribikram Kundu,
Proc. of SPIE Vol. 7650, 765019 · © 2010 SPIE · CCC code: 0277-786X/10/$18 · doi: 10.1117/12.847677

the received response, and the received signal is compared against a baseline to determine whether or not damage exists in the system.

To design a Lamb wave system, it is important to determine an optimal driving frequency for the structure under test. The excitation waveform also plays an important role in determining the effectiveness of a Lamb wave system. One of the most commonly employed excitation waveforms is a tone burst sine wave with a Hanning window, which is a raised-cosine with a roll-off factor of 1. Because a Hanning windowed sinusoid has low bandwidth, the generated Lamb waves are limited to their fundamental modes [4]. Figure 1 shows the excitation waveform used for our experiments, in both the time domain and the frequency domain.

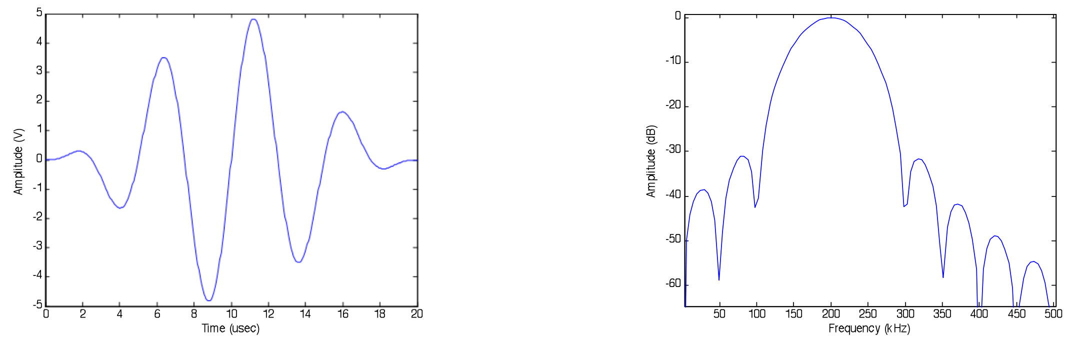


(a) Excitation Waveform in time domain (b) Normalized Frequency Spectrum

Figure 1: 200kHz excitation waveforms

In previous Lamb wave experiments involving an ADC, a discrete wavelet transformation (DWT) was used to reduce noise [5-7]. Equation (1) shows the mathematical representation of the discrete wavelet transform.

$$W_{\Psi}(j,k) = \sum_{j}\sum_{k} s(n)2^{-j/2}\Psi_{j,k}(2^{-j}n-k) \tag{1}$$

$\Psi_{j,k}$ is defined as the mother wavelet and has finite energy. In previous experiments, the excitation waveform has been used as the mother wavelet. By setting the dilation coefficient j=0 in (1), the DWT represents the correlation between the excitation signal and sensed signal.

To calculate the difference between separate runs, the following detection metric (DM) has been used. This detection metric calculates the total percent difference between the baseline waveform and the current waveform.

$$DM = \frac{\sum_{i}\left|WT_{current}(i) - WT_{baseline}(i)\right|}{\sum_{i}\left|WT_{baseline}(i)\right|} \tag{2}$$

The detection metric for an undamaged structure is ideally 0, and increases based on the amount of damage detected in a structure. $WT_{current}$ and $WT_{baseline}$ denote the DWT of the sensed and baseline waveforms, respectively. |x| denotes the absolute value of x.

### 2.2 Motivation

The primary motivation for this experiment is to reduce the overall power requirements of a Lamb wave system through elimination of the system's ADC. According to the datasheet, the ADC integrated into the TI TMS320F2812 DSP used in this experiment consumes over 120 mW when operating at the full speed [1]. We propose to replace this ADC with two comparators, whose combined power dissipation ranges from 2 mW typical to a maximum of 7.2 mW [8]. In addition, this method simplifies the processing required by the DSP. A DWT is no longer necessary in our proposed method, and all processing complexity is now on the order *O(n)*. This reduces the execution time of the DSP algorithms, which in turn reduces the energy usage of the DSP. In addition, the reduced power consumption makes it simpler to integrate multiple types of SHM tests into a single device, which is suggested in [9] as a method to increase the effectiveness of an SHM system.

# 3 PROPOSED METHOD

## 3.1 Elimination of ADCs

The ADC of a Lamb wave system captures the magnitude of the response signal at the sampling instance, and the magnitude value for an $n$-bit ADC is quantized to $2^n$ levels with a uniform distance between two adjacent levels. Our method is to quantize a value into three levels, values above a high threshold value are denoted as 1, values below a low threshold value are denoted as -1, and values in-between the two threshold values are denoted as 0. We use two comparators: an upper comparator sets the high threshold value and a lower comparator the low threshold value. The diagram for our system is shown in Figure 2.

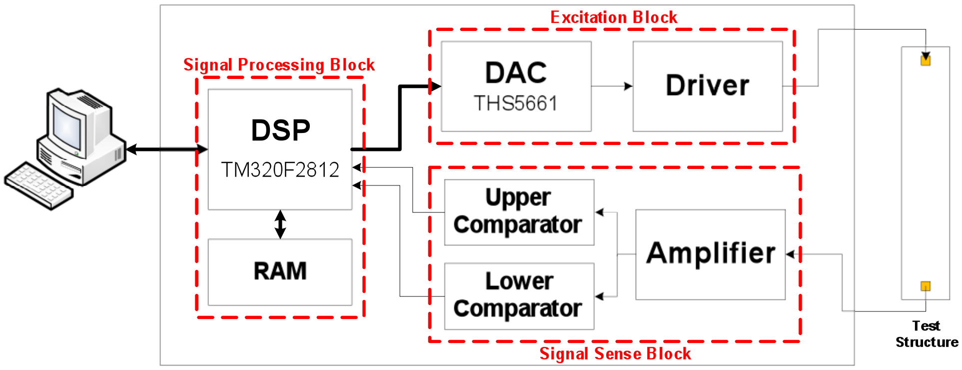


Figure 2: Block diagram of our Lamb wave system

The use of two comparators offers critical advantages over one comparator besides smaller quantization errors. The two comparators form a dead zone which decreases the effect of low-amplitude noise. Further, it is possible to set up the thresholds in an asymmetric configuration, where the high threshold has a different magnitude than the lower threshold. This allows the system to differentiate two separate amplitudes of the received signal. Figure 3 illustrates asymmetric threshold values.

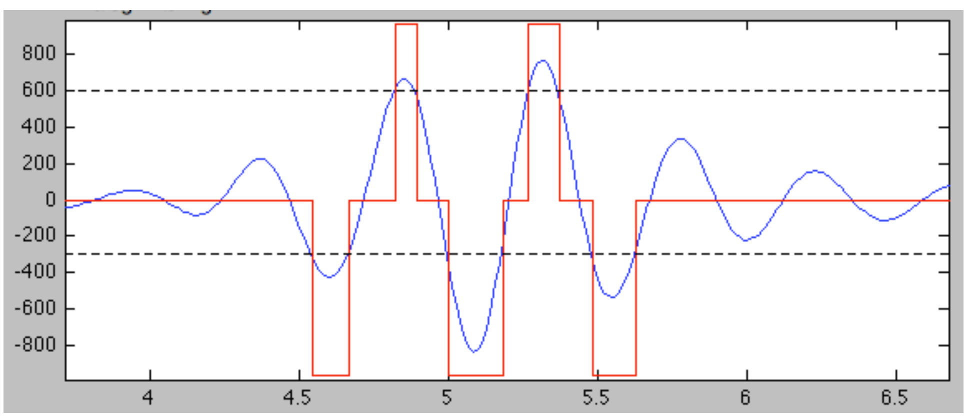


Figure 3: An example of asymmetric thresholds

## 3.2 Noise Reduction

When a signal level is near the threshold level of a comparator, the comparator's output is sensitive to noise, as illustrated in Figure 4. The cluster of two pulses around times 2.78 and 2.80 in this figure are due to noise. This kind of noise has been eliminated for our system by running the same operation eight times and determining the values through a majority vote.

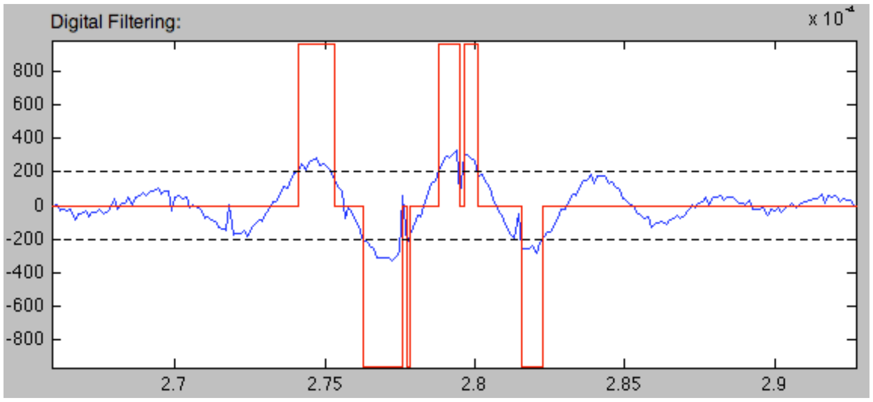


Figure 4: Impact of noise on a signal with signal levels around the threshold values

### 3.3 Prototype

The prototype for our comparator based system leverages our previous prototype for Lamb wave SHM [5]. The prototype is based on the TMS320F2812 DSP evaluation board. The DSP holds the digital excitation waveforms in memory, and the TI THS5661 DAC converts them to an analog waveform. This output is then low-pass filtered and amplified to drive a PZT patch. The received signal is amplified and biased by an op-amp and then applied to the inputs of two comparators. The MAX942 comparator from Maxim was chosen because of the fast rise time on its outputs and its low power consumption. The upper and lower threshold values are controlled by onboard potentiometers. The output from the comparator circuitry is applied directly to GPIO (General Purpose Input Output) ports on the DSP, completely bypassing the ADC integrated in the DSP. The average of eight runs is then taken and this is compared to the calculated baseline waveform. The detection metric in equation (2) is also used for this new system.

## 4 EXPERIMENTAL RESULTS

### 4.1 Experimental Setup

Our previous test structure described in [5] was reused for this experiment. Our experiments focused on a proof of concept for our comparator based system. The test structure is a 36" x 36" x 0.063" aluminum plate with PZT transducers mounted in a 12" x 12" square in the middle of the plate. Each PZT is 0.5" in diameter and 0.01" thick and is bonded to the aluminum plate using super glue. Figure 5 shows the test structure used for our experiments.

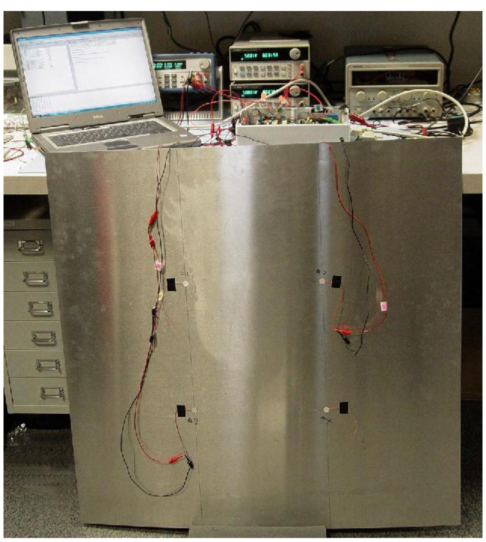

(a) Test Set-up

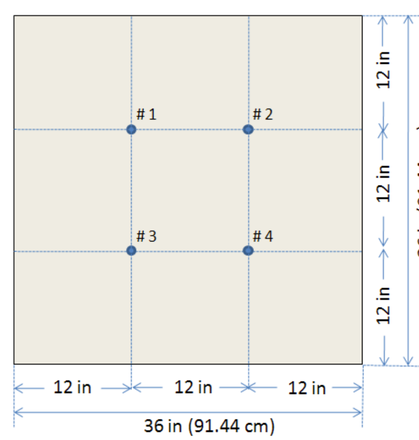


(b) Dimensions of the Plate

Figure 5: Test structure used

All experiments were performed between test points #2 and #4. The excitation frequency was set to 200 kHz, which was found previously as a suitable frequency for this plate [5]. The DSP was programmed to sample the response as fast as possible, which was approximately 5.5 MSPS. Since the DSP used for our experiments does not support Direct Memory Access (DMA), sampled values from the GPIO ports were copied into memory via a software means. Due to the speed overhead associated with use of timers and interrupt handlers, the DSP was programmed to repeatedly read values on GPIO ports in a loop instead of being triggered by timers. It should be noted that a finer control on the sampling frequency could be obtained through the use of DMA.

### 4.2 Comparator Waveforms

The MAX942 comparators used for our prototype are capable of producing a rise time of 9 ns, but the rise time was slowed to approximately 130 ns to prevent ringing in our prototype. A capacitor was added to the output of the comparator for this purpose, and the increased rise time offers a good compromise between speed and signal integrity. The increased rise time of the comparator also filters out very short noise pulses. Figure 6 shows a scope capture of the upper threshold comparator output versus the sensed waveform. Channel 1 shows the received waveform which has been amplified and biased. Channel 2 shows the output of the upper threshold comparator when connected to the signal from Channel 1.

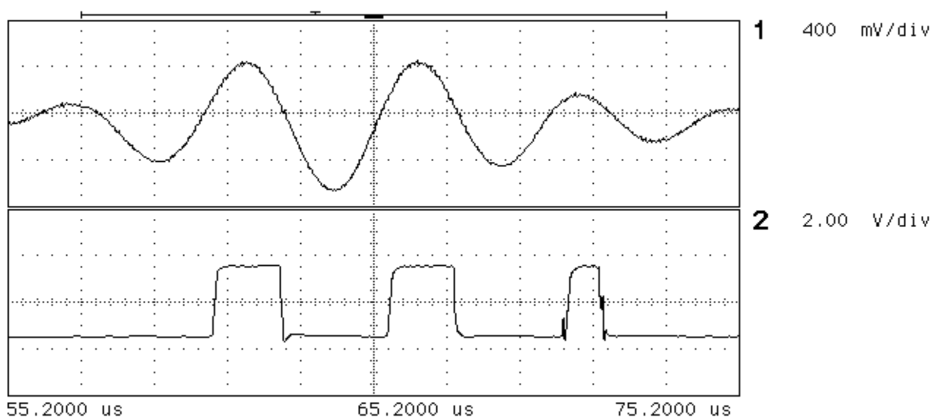


Figure 6: Time response of the upper threshold comparator

### 4.3 Calculated Detection Metrics

A baseline value is established by averaging the first eight runs. The system runs eight more times, and then a detection metric is calculated based on the average value of these eight runs. This calculated damage metric is labeled as "HEALTHY." A piece of clay is then introduced between points #2 and #4 in Figure 5 (b) to simulate damage. The system runs eight more times, and the detection metric labeled as "DAMAGED" is calculated. Both of these metrics are displayed in Table 1.

The peak-to-peak sensed voltages at the input of the comparators are 1.0 V to 2.1 V in our experiments, with a DC bias of 1.55 V. Since the detection metrics are affected by threshold values, we experimented with several different threshold values. Table 1 (a) shows damage metrics, where both the upper and lower threshold values are set to identical values ranging from ± 0.05 V to ± 0.25 V of the DC bias. The ratio of the HEALTHY detection metric to the DAMAGED detection metric ranges from 4.4 to 7.6 for the five different threshold values. We made two observations from this experiment: the ratios are sufficiently large to detect damage with high confidence, and the high ratios verify that the proposed method to replace ADCs with comparators works. Second, the ratio of the two metrics is quite sensitive to threshold values, and proper threshold values may be determined experimentally for a given set of damages. Note that the ratio increases as the magnitude of the threshold values increases but drops off after a certain value.

Table 1 (b) shows detection metrics under asymmetric threshold values. The lower threshold value is fixed to -0.05 V, while the upper threshold value varies from +0.1 V to +0.25 V. Using asymmetric threshold values, specifically a higher upper threshold magnitude than the lower threshold magnitude, was found to increase the ratios of the damage metrics significantly. The ratios range from 7.5 to 10.9 under these asymmetric threshold values.

Table 1 (c) shows detection metrics under another set of asymmetric threshold values. The low threshold value is fixed to -0.15 V, while the upper threshold value varies from +0.05 V to +0.25 V. The highest attained ratio of 13.2 is obtained for the -0.15/+0.2V run. However, detection metrics were found to vary less predictably as compared to Table 1 (b).

Table 1: Detection metrics calculated under various threshold levels

(a) Symmetric threshold values

| **Thresholds** | **-0.05/+0.05 V** | **-0.1/+0.1 V** | **-0.15/+0.15 V** | **-0.2/+0.2 V** | **-0.25/+0.25 V** |
|---|---|---|---|---|---|
| HEALTHY | 0.039 | 0.037 | 0.026 | 0.030 | 0.039 |
| DAMAGED | 0.170 | 0.186 | 0.176 | 0.228 | 0.210 |
| **Ratio** | 4.4 | 5.0 | 6.8 | 7.6 | 5.4 |

(b) Asymmetric threshold values with the low threshold value -0.05 V

| **Thresholds** | **-0.05/+0.1 V** | **+-0.05/+0.15 V** | **-0.05/+0.2 V** | **-0.05/+0.25 V** |
|---|---|---|---|---|
| HEALTHY | 0.032 | 0.030 | 0.024 | 0.029 |
| DAMAGED | 0.240 | 0.250 | 0.261 | 0.238 |
| **Ratio** | 7.5 | 8.3 | 10.9 | 8.2 |

(c) Asymmetric threshold values with the low threshold value -0.15 V

| **Thresholds** | **-0.15/+0.05 V** | **-0.15/+0.10 V** | **-0.15/+0.2 V** | **-0.15/+0.25 V** |
|---|---|---|---|---|
| HEALTHY | 0.035 | 0.040 | 0.018 | 0.017 |
| DAMAGED | 0.257 | 0.189 | 0.238 | 0.188 |
| **Ratio** | 7.3 | 4.7 | 13.2 | 11.1 |

# 5 CONCLUSION

The analog-to-digital converter (ADC) of a Lamb wave system is responsible for converting the received analog data into a format that can be processed by a processor. The power requirements for a high speed ADC as well as the processing requirements necessary to handle this amount of data greatly increase the total power requirements for a Lamb wave SHM system. Elimination of an ADC can therefore significantly reduce overall power dissipation of a Lamb wave system.

In this paper, we proposed a method to eliminate the ADC of a Lamb wave system, in which the ADC is replaced by two comparators. Our method is to quantize a sampled signal value into three levels with two comparators rather than into $2^n$ levels with an n-bit ADC. We presented experimental results performed with our prototype, and these experimental results indicate that the proposed method is effective at detecting simulated damage on aluminum plates.

# 6 ACKNOWLEDGEMENTS

We are thankful to Mr. Jeong Ki Kim for his assistance in completing the experiments reported in this paper.

# REFERENCES

[1] "SPRS174P - TMS320F2812 Datasheet," (2009). http://focus.ti.com/docs/prod/folders/print/tms320f2812.html

[2] R. A. Swartz, E. Flynn, D. Backman et al., "Active Piezoelectric Sensing for Damage Identification in Honeycomb Aluminum Panels," Proceedings of 24th Intl. Modal Analysis Conference, (2006).

[3] J. R. Wait, G. Park, H. Sohn et al., “Plate Damage Identification Using Wave Propagation and Impedance Methods,” Proceedings of SPIE, 5394(53-65), (2004).
[4] J. G. Proakis, and D. G. Nanolakis, [Digital Signal Processing] Prentice Hall, (2007).
[5] J. K. Kim, D. Zhou, D. S. Ha et al., "A practical system approach for fully autonomous multi-dimensional structural health monitoring." 7292, 72921L, (2009).
[6] S. Legendre, D. Massicotte, J. Goyette et al., ““Wavelet-Transform-Based Method of Analysis for Lamb-Wave Ultrasonic NDE Signals,” IEEE Trans. on Inst. and Meas., 49(3), 524-530 (2000).
[7] H. P. Sohn, W. G., J.R., N. P. Limback et al., “Wavelet-based active sensing for delamination detection in composite structures,” Journal of Smart Materials and Structures, 13, 153-160 (2004).
[8] "19-0229 - High-Speed, Low-Power, 3V/5V, Rail-to-Rail, Single-Supply Comparators," (2009). http://www.maxim-ic.com/quick_view2.cfm/qv_pk/1220
[9] A. Raghavan, and C. E. S. Cesnik, “Review of Guided-wave Structural Health Monitoring,” The Shock and Vibration Digest, 39(2), 91-114 (2007).